An Approach to Suppress RFI in Ultrawideband Low Frequency SAR

Viet T. Vu, Thomas K. Sjögren, Mats I. Pettersson and Lars Håkasson
Blekinge Institute of Technology (BTH)
37225 Ronneby, Sweden
Email: viet.thuy.vu@.bth.se

***Abstract*— The paper proposes an approach for the Radio Frequency Interference (RFI) suppression in ultrawideband (UWB) low frequency Synthetic Aperture Radar (SAR). The basis of the approach is an Adaptive Line Enhancer (ALE) controlled by the Normalized Least Mean Square (NLMS) algorithm. The proposal is tested successfully on the simulated CARABAS-II data.**

I. Introduction

Applications of Synthetic Aperture Radar (SAR) are found mainly in geosciences and remote sensing. SAR systems utilizing large fractional bandwidth and wide antenna beamwidth, which are interpreted as ultrawideband (UWB), have shown the ability to image large ground scenes with high resolution and facilitate change detection in dense forested areas or under camouflage at low frequencies. Such application is of interest to both military and civilian end-users.

UWB SAR data processing faces a number of challenges due to the unsuitability of using narrowband and narrowbeam approximations. The choice of SAR processing algorithm, coherent integration angle, sidelobe control and motion compensation are known as the challenges in UWB SAR processing [1] and have attracted much attention. Another challenge in UWB SAR data processing is known as Radio Frequency Interference (RFI). Considering RFI as a challenge in UWB SAR data processing is straight ahead as the possibility to be affected by RFI sources is directly proportional to the signal bandwidth and antenna beamwidth. However, there have not been many publications focusing on this technical issue. This may be explained by the dependence of it on the operating frequency of the SAR systems and the ground scenes of the field campaigns. For UWB SAR systems working at low frequencies and in extremely high thermal noise environments, RFI must be taken into account.

Let us consider an airborne UWB low frequency SAR system, for example CARABAS-II [2] which have been referred to in a large number of research works. This system operates in the lower VHF-band from 20 to 90 MHz and utilizes wide beamwidth dipole antennas (larger than 90^{o}). The field campaigns with CARABAS-II have been performed mainly in Sweden. The radar signal can therefore be affected by various shortwave bands (5.9-26.1 MHz), citizens' band (26.965 - 27.405 MHz), television channels 2-6 (54-88 MHz) and FM broadcast band (88-108 MHz). The measured power spectrum on the CARABAS-II recording data indicates that the radar signal is mainly influenced by tones at frequencies 22, 55, 60, 62 and 67 MHz [4]. This influence is seen to be extremely serious since the RFI energy is much higher than the reflected radar signal energy (up to 40 dB). To use the radar signal efficiently, an approach for RFI suppression is required.

One of the early researches on RFI suppression in wideband SAR signal (40 MHz) can be found in [3] where an adaptive filtering of RFI in baseband SAR signals has been experimented. A later research on this topic is presented in [4] where an approach in the frequency-domain with amplitude normalization is proposed and aims at low-frequency UWB SAR systems. Limitations of these approaches can mainly be found in Least Mean Square (LMS) adaptive filter, which may be sensitive to the non-stationary SAR scenes. In addition, the investigations are mainly restricted by the effects of RFI on raw radar echo.

The objective of this paper is to propose an approach to suppress RFI in UWB low frequency radar signal. The basis of the approach is an Adaptive Line Enhancer (ALE) [5]. The Normalized Least Mean Square (NLMS) algorithm [5], which avoids the sensitivity of the algorithm to the non-stationary ground scene, is suggested to use. Effects of RFI on radar signal and SAR image are investigated in detail. Evaluations of the proposal are based on the SAR image quality assessments such as Integrated Sidelobe Ratio (ISLR) and Peak Sidelobe Ratio (PSLR).

The paper is organized as follows. Section 2 presents the operation of ALE and the proposed approach for RFI suppression in UWB low frequency SAR. Simulation results and evaluations are given in Section 3. Section 4 provides the conclusions.

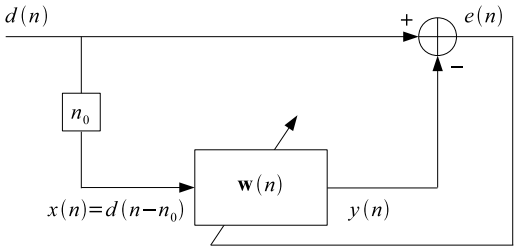

Fig. 1. ALE structure.

978-1-4244-5812-7/10/$26.00 ©2010 IEEE

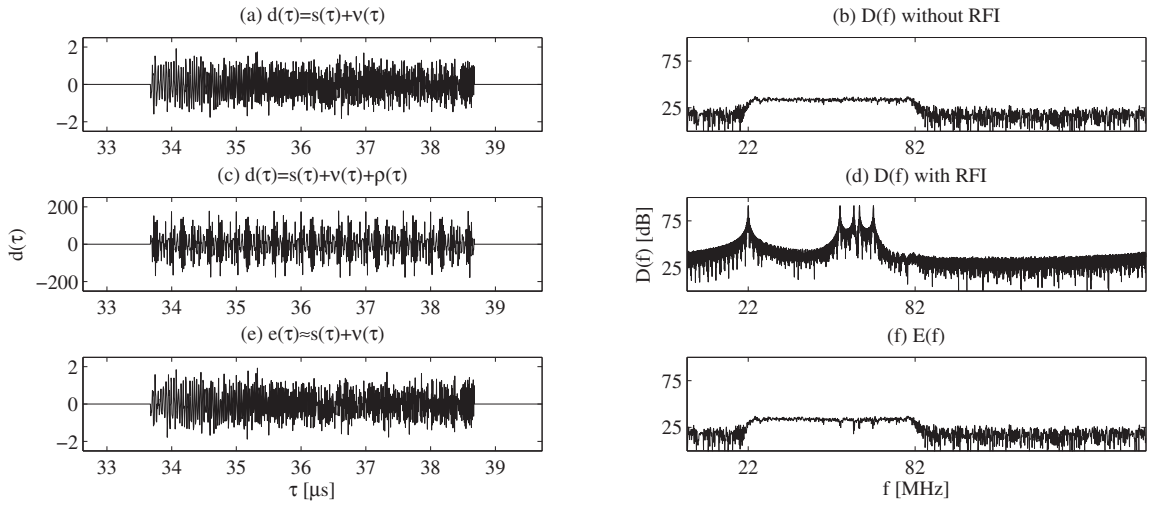

Fig. 2. An investigation of effects of RFI and ALE on the radar echo which is based on radar echo $d(\tau)$ and its associated power spectrum $D(f)$. (a) and (b) The UWB radar signal plus the noise signal with SNR of 3 dB. (c) and (d) The radar echo including the UWB radar signal, the noise signal and the RFI signal with ISR of 40 dB. (e) and (f) The UWB radar signal plus the noise signal estimated by ALE.

II. ALE AND AN APPROACH FOR RFI SUPPRESSION

ALE is interpreted as Adaptive Noise Cancellation (ANC) without a separate reference signal. The reference signal in ALE is generated by simply delaying the input signal. Figure 1 shows the structure of ALE. If the input of ALE is fed by a radar echo of a UWB SAR system, the input $d(n)$ includes the reflected UWB radar signal $s(n)$, the thermal noise signal $\nu(n)$ and the RFI signal $\rho(n)$. The input of ALE can be written in mathematical form as

$$d(n) = s(n) + \nu(n) + \rho(n) \tag{1}$$

The reference signal to the adaptive FIR filter $\mathbf{w}(n)$ is generated by delaying the input of ALE an integer number n_0 of samples and represented by

$$x(n) = d(n - n_0) \tag{2}$$

Since the input signal $d(n)$ is seen as a weakly stationary real stochastic process, the cross-correlation between the input signal $d(n)$ and the reference signal $x(n)$ is given by

$$r_{dx}(k) = E[d(n)\, x(n-k)], k \in Z \tag{3}$$

Assuming that n_0 is a minimum delay which de-correlate the UWB radar and the noise signals but not the narrowband RFI signal in the radar echo $d(n)$ and the reference signal $x(n)$, the cross-correlation (3) is equivalent of

$$\begin{aligned} r_{dx}(k) &= E[d(n)\, x(n-k)] \\ &= E[\rho(n)\, x(n-k)] \\ &= E[\rho(n)\, \rho(n-n_0-k)], k \geq 0 \end{aligned} \tag{4}$$

We also assume that the adaptive FIR filter converges to its Wiener filter coefficients. An estimate of the RFI signal is therefore given by the output signal of the filter

$$\rho(n) \approx y(n) = \mathbf{w}^T(n)\, \mathbf{x}(n) \tag{5}$$

where $\mathbf{w}(n)$ and $\mathbf{x}(n)$ are the filter coefficient vector and the reference signal vector of the L-order adaptive FIR filter, respectively. They can be represented in vector form as

$$\mathbf{w}(n) = [w_0(n)\ \ w_1(n) \cdots w_{L-1}(n)]^T \tag{6}$$

and

$$\mathbf{x}(n) = [x(n)\ \ x(n-1) \cdots x(n-L+1)]^T \tag{7}$$

The estimation error signal $e(n)$ in ALE will be an estimate of the UWB radar signal plus the noise signal

$$e(n) = d(n) - y(n) \approx s(n) + \nu(n) \tag{8}$$

An airborne UWB SAR system is usually associated with a long and nonlinear sensor trajectory. The high radiated energy RFI sources can appear anywhere and anytime in the illuminated ground scene. To avoid the sensitivity of the algorithm to the non-stationary ground scene, we propose to use NLMS to update the filter coefficients as

$$\mathbf{w}(n+1) = \mathbf{w}(n) + \frac{\beta}{\mathbf{x}^T(n)\, \mathbf{x}(n)} \mathbf{x}^*(n)\, [s(n) + \nu(n)] \tag{9}$$

with $0 < \beta < 2$. This algorithm allows updates of step size continuously and enables a better minimization of the mean square error in non-stationary environment compared to LMS.

III. SIMULATION RESULTS AND EVALUATIONS

In this section, we present some simulation results to illustrate and evaluate the proposed approach. The UWB SAR data is simulated according to the CARABAS-II parameters [2]. In the simulations, the processed frequency is in the range 22-82 MHz and the antenna beamwidth of 90º is used. For illustration purpose, the thermal noise is assumed to be Additive White Gauss Noise (AWGN) and the Signal to Noise Ratio (SNR) is 3 dB. The simulated ground scene is one point target located in the center of the SAR scene. The original

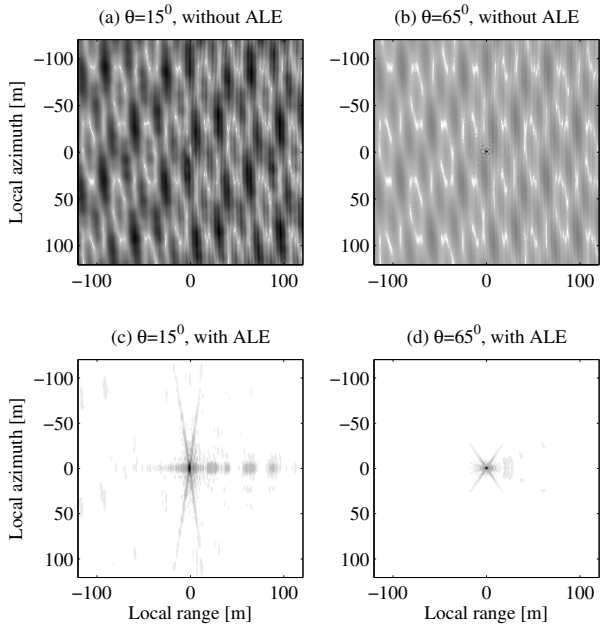

Fig. 3. An investigation of the RFI effects to SAR images and the performance of ALE in estimating UWB radar signal based on the SAR images. (a) and (b) The SAR images formed by the radar echo consisting of the UWB radar signal, the noise signal and the RFI signal and processed with $\theta = 15^{\text{o}}$ and $\theta = 65^{\text{o}}$. (c) and (d) The SAR images formed by the estimated UWB radar signal plus the noise signal and processed with $\theta = 15^{\text{o}}$ and $\theta = 65^{\text{o}}$.

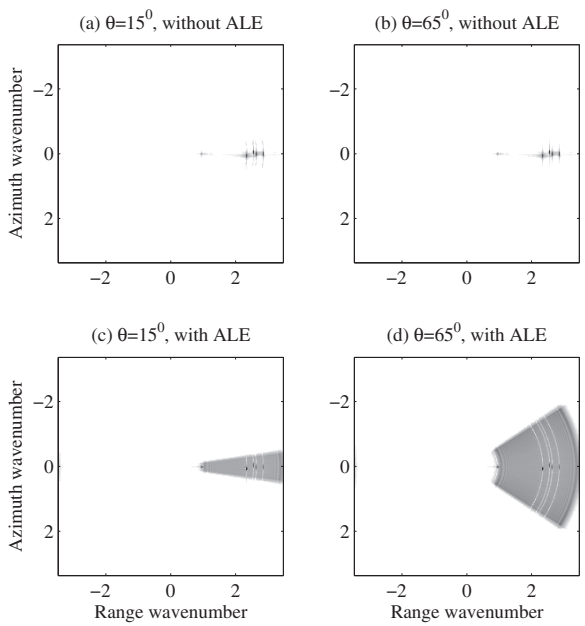

Fig. 4. An investigation of the RFI effects to SAR images and the performance of ALE in estimating UWB radar signal based on the SAR spectra. (a) and (b) The SAR spectra formed by the radar echo consisting of the UWB radar signal, the noise signal and the RFI signal and processed with $\theta = 15^{\text{o}}$ and $\theta = 65^{\text{o}}$. (c) and (d) The SAR spectra formed by the estimated UWB radar signal plus the noise signal and processed with $\theta = 15^{\text{o}}$ and $\theta = 65^{\text{o}}$.

UWB radar signal plus the noise signal and their associated power spectrum are plotted in Fig. 2(a) and 2(b), respectively. In these plots, we use the time τ and the frequency f axes instead of the sample axis n. The amplitude of the signals in the time-domain is given in dimensionless scale and the power spectrum in the frequency-domain in dB scale.

A. Effects of RFI

To investigate the effects of RFI, we assume that there exist five RFI sources in the simulated SAR scene and surrounding the point target. We also assume that these RFI sources are broadcasting stations operating in the frequencies of 22, 55, 60, 62 and 67 MHz. The Interference to Signal Ratio (ISR) is 40 dB. With this arrangement, the radar signal is considered to be affected seriously by RFI sources. The effects of RFI on the radar signal can be observed in Fig. 2(c) and 2(d). In the time domain, the UWB radar signal and the noise signal are totally hidden by the RFI signal. The amplitude of the RFI signal is higher about 100 times than the UWB radar signal. In the frequency-domain, the power spectrum is not as flat as the spectrum given in Fig. 2(b). The RFI power spectrum is dominant and the interference frequencies can also be seen clearly in the power spectrum.

In the next investigation, we use the radar echo consisting of the UWB radar signal, the noise signal and the RFI signal to form SAR images. Since UWB SAR is associated with long integration time to handle azimuth focusing, we process the radar echo with two different integration angles $\theta = 15^{\text{o}}$ and 65^{o}. This allows us examining the dependency of the RFI effects to SAR images on integration angle. Fig. 3(a) and 3(b) show the SAR images processed with $\theta = 15^{\text{o}}$ and 65^{o}, respectively. In both cases, the image quality is degraded significantly. The patterns caused by RFI appear everywhere in the SAR images. In the SAR image processed with $\theta = 15^{\text{o}}$, the point target in the center of the SAR scene is totally hidden by these patterns. Processing the radar echo with 65^{o}, the patterns caused by RFI can be partly suppressed and the point target in the center of the SAR scene can be seen. However, increasing integration angle should not be considered as an approach for RFI suppression due to the efficiency and the limitation of integration angle of any SAR system.

The RFI effects can also be observed on the SAR spectra given in Fig. 4(a) and 4(b). The typical UWB SAR spectra, i.e. a set of concentric circles spreading out over radar signal bandwidth and processed integration angle, are obscured by only some attenuated concentric circles corresponding to the interference frequencies and the positions of the RFI sources.

B. RFI suppression using ALE

In this demonstration, the proposed approach for RFI suppression is tested. An adaptive filter of order $L = 256$ in the ALE structure is selected for this test. The minimum delay to de-correlate the UWB radar signal and the noise signal is $n_0 = 1$. The normalized step size of the NLMS algorithm is experimentally chosen by $\beta = 0.015$.

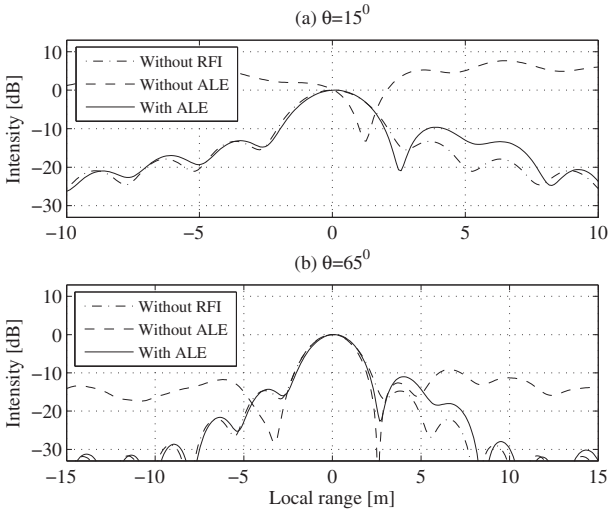

Fig. 5. An evaluation of the proposal is based on IR-SAR. (a) $\theta = 15^{\text{o}}$, (b) $\theta = 65^{\text{o}}$.

The estimated UWB radar signal plus the noise signal $e(\tau)$ and its associated power spectrum $E(f)$ are plotted in Fig. 2(e) and 2(f), respectively. The similarity between the original UWB radar signal plus the noise signal in Fig. 2(a) and the estimated UWB radar signal plus the noise signal using ALE Fig. 2(e) can be observed. The associated power spectrum of the estimated signals is considered to be flat. However, there may be some attenuations at the interference frequencies which can be recognized in the power spectrum given in Fig. 2(f).

The estimated UWB radar signal plus the noise signal are then used to form new SAR images. The SAR images in Fig. 3(c) and 3(d) correspond to the cases where the estimated signals are processed with the integration angles of 15^{o} and 65^{o}, respectively. The patterns caused by RFI almost disappear in the SAR images and the simulated ground scene with a point target in the center of the SAR scene can be distinguished, even with the small processing integration angle of 15^{o}. However, disturbance originated from the thermal noise and the remained effect of RFI are easier to be detected in the SAR image processed with 15^{o} compared to the one processed with 65^{o}.

Fig. 4(c) and 4(d) show the SAR spectra which are the typical UWB SAR spectra. The attenuations at the interference frequencies in the SAR spectra can also be identified.

C. Evaluations

The evaluation of the proposal is based on SAR image quality assessments such as ISLR and PSLR. The measurements are performed on the range vectors extracted from the peak intensities of the point target in the SAR images formed from the original UWB radar signal plus the noise signal, the radar echo consisting of the UWB radar signal, the noise signal and the RFI signal, and the estimated UWB radar signal plus the noise signal using ALE. The integration angles are also considered in these measurements. These vectors are plotted in Fig 5(a) and 5(b). These plots facilitate a visually detection of the serious RFI effect to the SAR images. As shown in Fig 5(a), the range vector extracted from the SAR image, that is formed from the radar echo and processed with $\theta = 15^{\text{o}}$, is totally different to the range vector extracted from the SAR image, that is formed from the original UWB radar signal plus the noise signal and processed with the same integration angle. The peak intensity of the point target is still lower than the peak intensity of the extracted range vector about 10 dB. This explains why the point target is totally hidden in the SAR image. The plots in Fig 5(b) can be interpreted as follows. RFI is partly suppressed due to the dependency of the RFI effects to SAR images on integration angle. Thank to this dependency, the point target in the SAR image processed with ($\theta = 65^{\text{o}}$) can be seen. The range vectors extracted from the SAR images, which have been formed from the estimated UWB radar signal plus the noise signal, are very similar to the range vectors extracted from the SAR images that have been formed from the original UWB radar signal plus the noise signal. The measurement results of ISLR and PSLR on the different extracted range vectors, which are summarized in the Table I, give us a better view about the performance of the proposed approach.

TABLE I
MEASUREMENT RESULTS

	$\boldsymbol{\theta = 15^{\text{o}}}$		$\boldsymbol{\theta = 65^{\text{o}}}$	
	ISLR	***PSLR***	***ISLR***	***PSLR***
Without RFI	26.3 dB	-13.3 dB	32.4 dB	-14.7 dB
Without ALE	-4.9 dB	7.6 dB	15.8 dB	-9.1 dB
With ALE	22.0 dB	-9.6 dB	26.8 dB	-11.1 dB

According to (4), the performance of ALE depends strongly on the ratio of the ability to de-correlate the UWB radar signal in the radar echo $d(n)$ and in the reference signal $x(n)$. In other words, it depends on the interrelation of the UWB radar signal bandwidth and the RFI signal bandwidth. In the environments where there exists RFI whose bandwidths are large enough to be also de-correlated by the minimum delay selection n_0, ALE might not work efficiently. The selections of β is critical to the convergence and stability of NLMS and therefore the RFI suppression result. A large selected value of β can result in faster convergence of NLMS. However, such selection may also lead to instability of the algorithm.

In the demonstrations, the ideal assumptions such as the simple SAR scene with a single point target and the RFI sources radiating the pure tones have been used. However, this approach also works in reality and have been tested successfully with the real CARABAS-II data [6].

A comparison between the proposed approach and the Linear RFI Filtering (LRF) technique [7], which is currently used in CARABAS-II data processing, is also provided in [6]. This comparative study shows that the performance of the proposed approach is very similar to the LRF technique.

IV. Conclusion

An approach to suppress RFI in UWB low frequency SAR is proposed in this paper. The proposal is based on the ALE structure which is controlled by the NLMS algorithm. The simulation results and the evaluations show the efficiency of the proposal. The RFI effects to the radar signal and SAR images are investigated.

Acknowledgment

The authors would like to thank the KK-Foundation for making this research project possible, and the support from Swedish Defence Research Agency, Saab Bofors Dynamics, Saab Microwave Systems and RUAG Aerospace Sweden.

References

[1] R. Goodman, S. Tummala, and W. Carrara, "Issues in ultra-wideband, widebeam SAR image formation," in *Proc. IEEE International Radar Conference*, Alexandria, VA, May 1995, pp. 479–485.

[2] A. Gustavsson, L. M. H. Ulander, B. H. Flood, P.-O. Frölind, H. Hellsten, T. Jonsson, B. Larsson, and G. Stenstrom, "Development and operation of an airborne VHF SAR system-lessons learned," in *Proc. IEEE IGARSS'98*, vol. 1, Seattle, WA, Jul. 1998, pp. 458–462.

[3] C. T. Le, S. Hensley, and E. Chapin, "Adaptive filtering of RFI in wideband SAR signals," *7th Annual JPL Airborne Earth Science Workshop*, Jet Propulsion Laboratory, Pasadena, CA, Jan. 1998.

[4] X. Luo, L.M.H. Ulander, J. Askne, G. Smith, and P.-O. Frolind, "RFI suppression in ultra-wideband SAR systems using LMS filters infrequency domain," *IET Electronics Letters*, vol. 37, no. 4, pp. 241–243, 2001.

[5] Monson H. Hayes: *Statistical sigital signal processing and modeling*, Wiley, 1996.

[6] V. T. Vu, T. K. Sjögren, M. I. Pettersson, L. Håkansson, A. Gustavsson, and L. M. H. Ulander, "RFI suppression in ultra-wideband SAR using adaptive line enhancer," *IEEE Geosci. Rem. Sens. Lett.*, accepted for publication.

[7] L. M. H. Ulander, and P.-O. Frölind "Precision processing of CARABAS HF/VHF-band SAR data," in *Proc. IEEE IGARSS'99*, vol. 1, Hamburg, Germany, Jun. 1999, pp. 47–49.